Adaptive Radio Resource Allocation for a Mobile Packet Service in Multibeam Satellite Systems

Kwangjae Lim, Sooyoung Kim, and Ho-Jin Lee

In this paper, we introduce an adaptive radio resource allocation for IP-based mobile satellite services. We also present a synchronous multibeam CDMA satellite system using an orthogonal resource sharing mechanism among downlink beams for the adaptive packet transmission. The simulation results, using a Ka-band mobile satellite channel and various packet scheduling schemes, show that the proposed system and resource allocation scheme improves the beam throughput by more than two times over conventional systems. The simulation results also show that, in multibeam satellite systems, a system-level adaptation to a user's channel and interference conditions according to user locations and current packet traffic is more efficient in terms of throughput improvement than a user-level adaptation.

Keywords: Multibeam satellite, mobile radio, adaptive allocation, radio resource, packet transmission.

I. Introduction

The geosynchronous orbit (GSO) satellite communication system with multiple spot beams and large satellite antenna(s) can provide high-rate services to small user terminals thanks to a large satellite antenna gain. It can also support a larger capacity than a system with a single global beam for the service area [1]. In the next-generation satellite systems for packet services, an efficient and adaptive radio resource allocation is essential for a high capacity and spectral efficiency. In particular, the allocation scheme for the forward (earth station to user) link is more important than that for the reverse (user to earth station) link because of an asymmetric bandwidth requirement of the IP-based packet services.

For a multibeam satellite system, we can consider a typical satellite-based CDMA cellular system [2], [3], where a full frequency reuse is applied as in terrestrial CDMA cellular systems. This approach, based on CDMA techniques, can provide for a high spectral efficiency by using different scrambling codes, such as pseudo noise sequences, for different beams in the same frequency band. In this paper, we refer to such a conventional multibeam satellite system as an *asynchronous* multibeam system. However, the adjacent beams generate the interbeam interference to the desired beam because of the imperfect orthogonality between the pseudo noise scrambling codes. The interference from other beams is more serious than in the terrestrial system because of the imperfect isolation of satellite antenna radiation patterns.

Meanwhile, in the multibeam GSO satellite system, we can easily synchronize all the downlink (satellite-to-user link) signals from a single satellite because the satellite is the only signal source. In such a satellite system using the *synchronous* multibeam, the beam signals received at a user are also

Manuscript received Feb. 17, 2004; revised Mar. 03, 2004.
This work was supported in part by the Korean Ministry of Information and Communication.
Kwangjae Lim (phone: +82 42 860 6523, email: kjlim@etri.re.kr) and Ho-Jin Lee (emali: hjlee@etri.re.kr) are with Digital Broadcasting Research Division, ETRI, Daejeon, Korea.
Sooyoung Kim (email: sookim@chonbuk.ac.kr) is with Division of Electronics & Information Engineering, Chonbuk National University, Jeonju, Korea.

synchronized regardless of the user location. Therefore, if the downlink beams are discriminated by orthogonal codes such as Walsh codes, we can decrease the interbeam interference. In [4], we introduced a multibeam satellite system using a synchronous transmission among the downlink beams and proposed a downlink radio resource allocation method for the proposed system. In this paper, we present an efficient adaptive scheme for packet transmission in the synchronous multibeam system and evaluate the performance of the adaptive scheme in a Ka-band mobile satellite channel.

Recently, much work on radio resource allocation problems has been devoted to the terrestrial third-generation systems and future wireless systems. The authors in [5] and [6] considered transmission power and rate allocation for multiple service classes on the reverse link in cellular CDMA systems, where it is assumed that the closed-loop power control (CLPC) is perfect and that the adjacent cell interference is given. Resource control for the forward link can be found in [5], which drives a signal-to-interference ratio (SIR) and rate control for data users under quality of service (QoS) constraints. These studies focused on a link adaptation, given channel information on each user and intercell interference. However, the received signal quality is affected by interference from adjacent cells, severely so when users are located at the cell boundary. Intercell interference is variable and depends on the instantaneous traffic and allocated transmission in the adjacent cells. In a multibeam satellite system, the interference from the adjacent beams is more serious because the path loss difference between beams mostly depends on the beam radiation pattern rather than on the distance.

The authors in [7] and [8] studied radio resource allocation in a time-division (TD) CDMA environment, where time division multiplexing (TDM) as well as code division multiplexing (CDM) were considered together. The optimum resource allocation problem in such a TD-CDMA system can be approached by dynamic programming, but it is known to be NP-complete [7]. For this reason, the authors in [7] and [8] proposed heuristic approaches as a sub-optimum solution. The authors in [9] proposed packet scheduling schemes from the perspective of QoS, assuming a given radio capacity. However, in real radio situations, the capacity is not fixed but varies according to the user distribution in multiple cells, the channel conditions of each user, and the transmission traffic in the home and surrounding cells (resulting in the interference).

In this paper, we propose adaptive resource allocation schemes for a multibeam satellite environment, where all beams share the same band. The scheme allocates the resources adaptively by considering the dynamically varying multibeam interference and the different channel conditions of each user.

In the next section, we start by describing the synchronous multibeam system for orthogonal resource sharing among downlink beams. In section III, we describe adaptive packet transmission methods for the synchronous multibeam system. In section IV, we show and discuss the performance results obtained by computer simulations using a Ka-band land mobile satellite channel and an IP web-browsing traffic model. In section V, we conclude this paper.

II. Synchronous Multibeam Satellite System

We consider a multibeam GSO satellite system as a radio access network for the next-generation mobile packet services. Figure 1 illustrates the multibeam satellite system providing IP packet services. Services for mobile users are linked to a terrestrial IP core network through a fixed earth station (FES) and satellite. The GSO satellite has to be equipped with a large directional antenna in order to provide high-speed services for nomadic and portable terminals equipped with a small antenna of which the diameter ranges from a few to tens of centimeters. The FES performs adaptive resource allocation on the downlink and is a gateway to link the user services to the terrestrial network. When the satellite has an on-board processing capability, it can perform the adaptive resource allocation. In this paper, we focus on the forward downlink (satellite-to-user link) because the uplink is configured by the FES with a large antenna and high power; however, the downlink is more vulnerable.

In the synchronous multibeam system [4], all the downlink signals from a satellite are synchronized in time and frequency domains. The downlink radio frame consists of multiple frequency/time slots in an FDM and TDM fashion.

In each time/frequency slot, the radio resource is subdivided by orthogonal spreading codes in a CDM fashion. A radio resource unit (RRU) is defined by a specific spreading code in a specific frequency/time slot. All beams share the orthogonal RRUs for packet transmission. Due to the synchronized transmission, every RRU is orthogonal to each other. A unique pilot symbol sequence for each beam is transmitted in a predefined portion of the frame. The pilot sequence is spread by a beam-specific pilot code.

In a slot, the traffic signal is spread by the orthogonal spreading codes, but it is not scrambled by a beam-specific pilot code. Therefore, due to the synchronized transmission on all of the beams, the transmission signals from different beams are orthogonal to each other if the beams use different spreading codes in the same slot. Due to the orthogonality between RRUs, the interbeam interference is minimized, which improves the system capacity. In the asynchronous multibeam system mentioned in the previous section, the

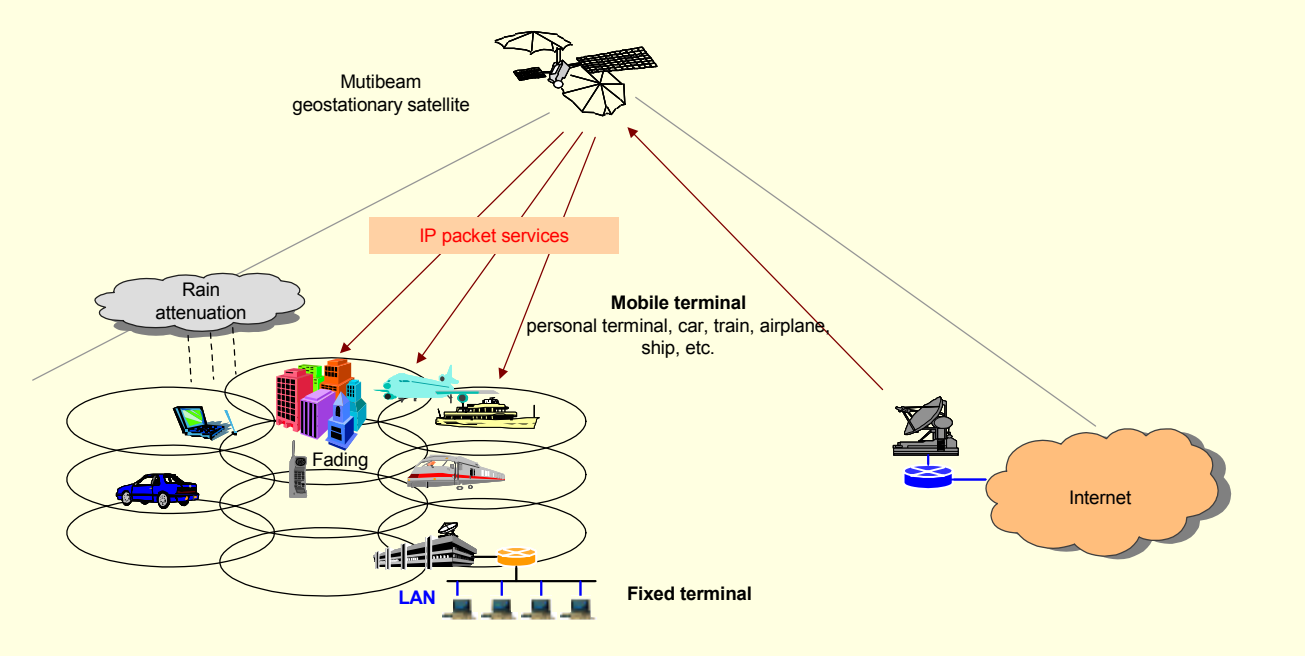

Fig. 1. A multibeam satellite system as a radio access network.

adjacent beams generate the interbeam interference to each other because the signals from different beams are scrambled by the beam-specific scrambling codes, and thus the beam signals are not orthogonal.

In mobile environments, the orthogonality between different spreading codes in the same frequency/time slot can be broken by time-dispersive multipath (frequency-selective) fading. In this paper, we consider imperfect RRU orthogonality as an interference factor between orthogonal spreading codes.

Under heavy load conditions, the number of RRUs available in a beam can be restricted because all beams share the RRUs. In order to avoid this resource limitation, the RRUs are reused if the distance between users serviced is sufficiently large so that the interbeam interference can be ignored. The radio resource allocation presented in [4] minimizes the interbeam interference by allocating and reusing the RRUs optimally. Moreover, the code limitation problem can be solved by using radio formats with a high spectral efficiency, such as 16-ary quadrature amplitude modulation (QAM). The use of high-rate modulation can reduce the number of RRUs required for packet transmission.

For the adaptive packet transmission, every user on a service measures the beam pilots and periodically reports the measured result to the FES through the reverse link. The user report includes the received power and signal-to-interference ratio (SIR) on the primary beam and adjacent beam pilots. The primary beam for a user means the one that currently provides packet services. Based on the reported link conditions, the resource management center in the FES performs a packet scheduling, selects the best resource for each packet transmission, and assigns the transmit power and radio format (modulation and coding type).

In satellite systems, a long propagation delay makes it difficult to adaptively allocate the frequency/time slot against fast frequency-selective fading because the correlation time of the faded signal is much smaller than the round trip delay. For this reason, we consider a link adaptation to slow fading such as shadowing. In this paper, we assume the user report is perfectly performed by reverse link transmission.

III. Adaptive Radio Resource Allocation

We deal with the complex resource allocation problem using a phased approach, where the allocation problem is divided into three sub-problems. The allocation procedure consists of three phases: packet scheduling, radio resource selection, and power and rate control. The center performs the allocation procedure in every radio frame.

1. Packet Scheduling

The first phase of the allocation procedure is the packet scheduling in which an allocation priority of the packet for each user is decided according to the user's channel state, the service class, and the required QoS delay. The priority of packet k at the head of a service queue for user u is calculated by

$$w_{u,k} = (c_u)^{a_1} \left(\gamma_{u,pilot}\right)^{a_2} \left(1/\gamma_{u,avg}\right)^{a_3} \left(1 + t/t_k\right)^{a_4}, \qquad (1)$$

where c_u, $\gamma_{u,\text{pilot}}$, $\gamma_{u,\text{avg}}$, t, and t_k represent the grade of service class, the latest pilot SIR on the primary beam, the average of the pilot SIR for the primary beam, the current time, and the time deadline given by the QoS requirement, respectively. The exponents of a_1, a_2, a_3, and a_4 (all ≥ 0) are used for controlling the dependency on each factor in the priority calculation.

This scheduling can differentiate the QoS according to the service requirements. The instantaneous radio capacity dynamically changes according to the current channel conditions of the active users. The scheduling determines which packet is transmitted first and how many resources are required, while the following resource selection determines which resources are best and how many resources are available for the scheduled packet.

Using (1) we can make various scheduling schemes. For example, by setting a_1=0, a_2=1, a_3=0, and a_4=0, we can give the highest priority to the packets for a user under the best channel conditions. Table 1 shows the exponent value settings for five exemplary scheduling schemes. In section IV, we will consider four types of packet scheduling for giving priority to the packet: i) with the maximum received SIR (Max SIR), ii) with the best channel condition compared with the average channel condition (SIR/Avg), iii) with the highest urgency and the maximum received SIR (SIR* Delay), and iv) with the round-robin method (Round-robin).

Table 1. Exponent values of (1) for various scheduling schemes.

Type	a_1	a_2	a_3	a_4
Class-based	1	0	0	0
Max SIR	0	1	0	0
SIR/Avg	0	1	1	0
SIR*Delay	0	1	0	2
Round-robin	0	0	0	0

2. Radio Resource Selection

The second phase of the allocation procedure is RRU selection. The procedure selects a set of the best RRUs for the packet transmission with the highest allocation priority. The best RRU means an RRU in which the smallest power is required for the packet transmission. This leads to the lowest interference to other packet transmissions already allocated and thus makes it possible to use radio resources maximally.

The received SIR, $\gamma_{u,(b,s,m)}$, transmitted through an RRU (b, s, m) of beam b, frequency/time slot s, and spreading code m, can be defined by

$$\gamma_{u,(b,s,m)} = SF \frac{p_{b,s,m} g_{b,u}}{I_{b,u,s} + Z_{b,u,s} + N_{noise}}, \tag{2}$$

where SF, $p_{b,s,m}$, $g_{b,u}$, $I_{b,u,s}$, $Z_{b,u,s}$, and N_{noise} represent spreading gain, transmit power used for the packet transmission in RRU (b, s, m), downlink gain between beam b and user u, intrabeam interference, interbeam interference, and background noise power, respectively. The link gain includes path loss, fading, and satellite and user antenna gains on the forward downlink.

The transmit power required for satisfying a target SIR γ_u^* can be written by

$$p_{b,s,m} = \frac{\gamma_u^*}{SF \phi_{u,(b,s,m)}}, \tag{3}$$

where $\phi_{u,(b,s,m)}$ denotes a gain-to-interference ratio (GIR) and is defined by

$$\phi_{u,(b,s,m)} = \frac{g_{b,u}}{I_{b,u,s} + Z_{b,u,s} + N_{noise}}. \tag{4}$$

From (3), we can observe that minimizing the required power means maximizing the GIR. Therefore, the procedure selects the best RRU (b^*, s^*, m^*) for each packet transmission by

$$(b^*, s^*, m^*) = \arg\max_{(b,s,m) \in V} \phi_{u,(b,s,m)}, \tag{5}$$

where V is a set of RRUs available in the current frame.

The downlink gain in (5) is estimated from the user report on received beam pilot power. Because of a practical limitation on user reporting, the link gains for all of the adjacent beams may not be available to the center. Therefore, we assume that users report only the measurement on the beam pilots whose SIR satisfies $\gamma_{\text{pilot},b} \geq \gamma_{\text{pilot, primary}} / \lambda_{\text{report}}$, where $\gamma_{\text{pilot, primary}}$ and λ_{report} denote the pilot SIR of the primary beam and the pilot SIR threshold ratio for the user reporting, respectively. We refer to such beams as active beams for the user. The link gains not included in the user report are estimated by a ratio of the primary link gain and the pilot SIR threshold. The link gain $g_{j,u}$ between beam j and user u is estimated by

$$g_{j,u} = \begin{cases} p_{\text{pilot},j} / p_{\text{pilot},j,u}, & \text{for } j \in B_{\text{report},u} \\ g_{\text{primary},u} / \lambda_{\text{report}}, & \text{for } j \notin B_{\text{report},u} \end{cases}, \tag{6}$$

where $p_{\text{pilot},j}$, $p_{\text{pilot},j,u}$, $g_{\text{primary},u}$, and $B_{\text{report},u}$ are the pilot transmit power used for beam j, the received pilot power of beam j at user u, the link gain estimated for the primary beam of user u, and the set of adjacent beams for user u, respectively. The pilot SIR threshold ratio λ_{report} gives a trade-off between system

throughput and reporting overhead. When λ_{report} is small, and thus the size of the set for the adjacent beams is small, the system will overestimate the link gains not included in the report. This again makes the system overestimate the interbeam interference and results in a decrease of the system throughput.

The interferences in (5) are estimated by using the reported link gain and the transmit power already allocated in the primary and adjacent beams as follows:

$$I_{b,u,s} = \kappa_{oc} \sum_{\substack{(b,s,i)\in V_{b,s}, \\ i\neq m}} p_{b,s,i} g_{b,u} \ , \quad \text{and} \tag{7}$$

$$Z_{b,u,s} = \kappa_{oc} \sum_{\substack{j\in B_b, \\ j\neq b}} \sum_{\substack{(j,s,i)\in V_{j,s}, \\ i\neq m}} p_{j,s,i} g_{j,u} + \sum_{\substack{j\in B_b, \\ j\neq b}} p_{j,s,m} g_{j,u}, \tag{8}$$

where B_b and $V_{b,s}$ are the set of beams adjacent to beam b and the set of RRUs in slot s of beam b, respectively. The term κ_{oc} denotes an interference factor representing the power-normalized interference between orthogonal spreading codes in frequency-selective fading. We can expect a perfect orthogonality of κ_{oc}=0 between the different orthogonal spreading codes if the channel is not frequency-selective. However, in the multipath propagation channel, there is no orthogonality between delayed multiple replicas of signals. In this case, the interference factor is larger than zero ($0<\kappa_{oc}<1$).

A non-zero κ_{oc} depends on the chip rate, the delay spread of the multipath fading channel, and the detection scheme adopted in the user terminals.

In order to reduce complexity in the RRU selection, the scope of the GIR investigation is limited to the RRUs of the primary beam. For the same reason, in the estimation of the interbeam interference by (8), we only consider the interference from the adjacent beams close to the primary beam instead of estimating the interference from all beams. In a coverage model consisting of hexagonal cells, the neighboring beams in the first and second rings around the primary beam are considered as adjacent beams. According to the RRU selection by (5), the use of the same code between the different beams is automatically avoidable because the same code interference overwhelms the other interference components in the GIR estimation by (4).

3. Power and Rate Control

The third phase of adaptive transmission allocation is power and rate control. The required transmit power can be adjusted by the distributed closed-loop power control (CLPC) which is commonly used in terrestrial CDMA cellular systems [10]. However, CLPC is inappropriate for adaptive packet transmission in a satellite system because of the long round-trip delay and intermittent transmission characteristic of packet services. As far as interbeam interference is concerned, it is uncertain that the interference condition will be preserved because the interference from the adjacent beams can be changed by the dynamic allocation according to packet traffics. Moreover, in a slotted radio frame by TDM and FDM, the center may change the slot used for the current packet transmission according to the RRU selection procedure. In the changed slot, the interference situation will be different from that in the previous packet transmission. Such problems mainly come from the distributed control manner in which the control procedure has no information on the interference variation.

To solve those problems, we use a centralized power control algorithm based on the estimated link gains and interference. The transmit power required for the packet transmission in a selected RRU is computed by the following iterative algorithm:

For steps $n = 0, 1, \ldots, N_{itr}-1$,

$$p_{b,s,m}(n+1) = \frac{\gamma_u^* / SF}{\phi_{u,(b,s,m)}(n)}, \ (b,s,m) \in V_{b,s}. \tag{9}$$

Here, N_{itr} and γ_u^* are the maximum iteration number and the SIR required to satisfy a bit error rate (BER) specified by the user service. This algorithm uses the estimated GIR from (4), and the transmit power is updated at every iteration for the packets allocated in slot s. The FES performs this whole iteration in a centralized operation and produces the minimum power value to satisfy the required SIR for each packet.

In the power computation above, the required SIR depends on the modulation and coding scheme used for the packet transmission as well as the required BER. The system selects a radio format according to the availability of radio resources (RRU and power) by the following three rules. First, if there is an available resource, the system allocates a basic format for the packet transmission. Basic modulation is one that requires the smallest SNR per bit for satisfying a specific BER, such as quadrature phase shift keying (QPSK). Second, when the transmit power is insufficient to satisfy the required SIR using the basic format, the system allocates a low-rate format, such as QPSK with a low code rate or symbol repetition. Third, when there is no available RRU for the current packet, the center searches a packet transmission with the largest GIR among the pre-allocated packet transmissions and changes the radio format to a high-rate one, such as 16-ary QAM. By doing this, the system can obtain empty RRUs available for the current packet.

IV. Simulation Results

We evaluated the performance of the proposed adaptive radio resource allocation methods using computer simulations. A service area consists of wrap-around hexagonal cells in order to avoid a border effect, and each cell is covered by a spot beam. Since we focused on the forward downlink, we assumed the perfect forward uplink and reverse link. To avoid a dependency on a specific user distribution over the service area, we averaged out the results from more than one hundred simulation runs with different user positions. The antenna radiation pattern for each beam was generated by the model in [3]. The radius of a cell serviced by a spot beam can be determined by an off-axis loss at the beam edge with respect to the maximum antenna gain. Table 2 shows the main simulation parameters.

We used a mobile satellite channel model for a Ka-band suburban channel in [11]. The received signal level is characterized by an embedded Markov chain with three states: the line-of-sight (LOS) condition, the moderate shadowing condition, and the deep shadowing condition. These fading states are generated by the steady state probabilities and state transition probabilities for a suburban environment, as presented in [11]. The state duration is modeled by an exponential distribution with average duration t_{fade}, given by $t_{fade} = d_{corr}/v_{user}$, where d_{corr} and v_{user} are the fading correlation distance and user speed. The Ka-band link is vulnerable to rain attenuation, but this is excluded in the simulations of this paper and left to a future study. In this paper, we mainly concentrated on the adaptive transmission to mobile fading and interference.

The packets for each user service are generated by an IP web-browsing model [12]. For simplicity, we applied a single type of service for all users. A selective-repeat automatic retransmission query was applied and the retransmission was limited to four times.

In the simulations, intrabeam interference from the primary serving beam and interbeam interference from all of the surrounding beams are considered as in (7) and (8), respectively. For the radio resource allocation algorithm, we limited the set of adjacent interfering beams in order to reduce the algorithm complexity, but all beams are considered for the actual received SIR computation. Note that all cells are active, and thus they allocate packet transmissions according to traffic request and generate dynamic interference to each other.

Successful packet reception by a user is decided according to the packet error rate (PER) on the current fading state and the received SIR. The PER, P_{PER}, is calculated by $P_{PER} = 1 - (1 - P_{BER})^L$, where L is the packet length in bits. The P_{BER} denotes a bit error rate and depends on the modulation format used, the current fading state, and the corresponding Rician K-factor. The BER tables for the modulation formats were obtained from a preliminary link-level simulation. QPSK is considered for the basic modulation format, and 8-ary PSK and 16-ary QAM are considered for the high-rate modulation formats. For

Table 2. Simulation parameters.

Simulation parameters	Values
Downlink carrier frequency	20 GHz
Channel bandwidth	5.12 MHz
Number of spot beams	19
Maximum beam power	30 W
Downlink free-space loss	210 dB
Maximum beam antenna gain	64.4 dBi
User antenna gain	19.4 dBi
Off-axis loss at beam edge	6 dB
Background noise power	-102 dBm
Round trip delay	0.5 s (bent-pipe)
Frame duration	20 ms
Number of slots	10
Number of spreading codes	16
User speed	Uniform in 0 to 120 km/h
Fading correlation distance (d_{corr})	5 m
Interference factor (κ_{oc})	0.05
Pilot SIR threshold ratio (λ_{report})	20 dB
Report period (T_m)	100 ms
Power control iteration number (N_{itr})	5

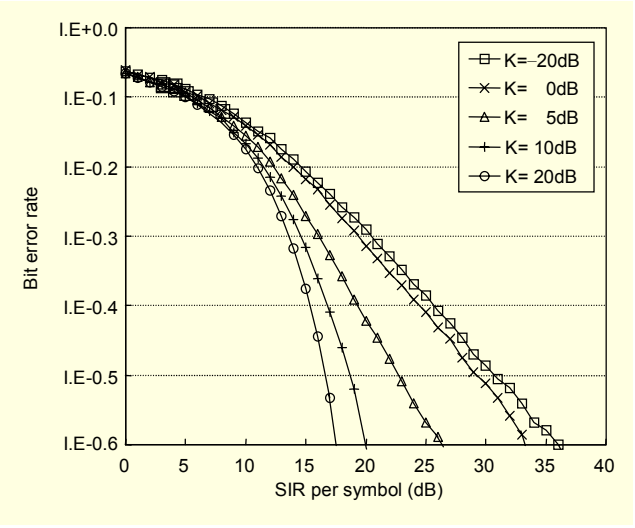

Fig. 2. BER performance of the 16-ary QAM under the uncorrelated Rician fading channel. The parameter K denotes the Rician K-factor.

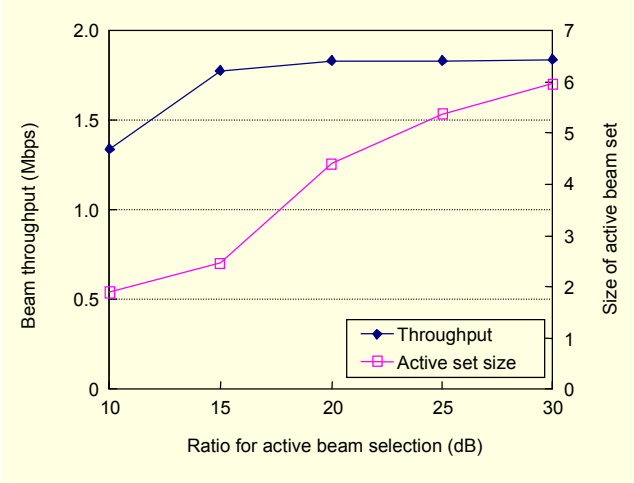

Fig. 3. Beam throughput and active beam set size according to pilot SIR threshold ratio (Max SIR scheduling, 400 users).

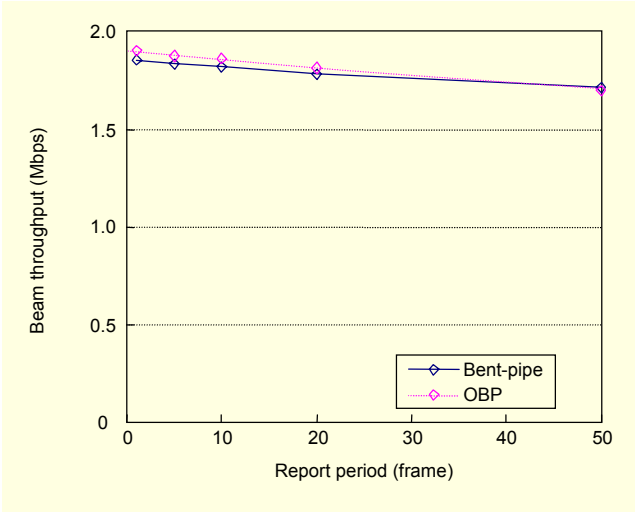

Fig. 4. Beam throughput according to the user report period (Max SIR scheduling, 400 users).

the low-rate modulation formats, we used the QPSKs using a symbol repetition of x times, where $x = 2$, 4, or 8. Hence, in our simulations, six different transmission rates per RRU with a range of 8 kbps to 128 kbps can be selected for the power and rate control. For example, Fig. 2 shows the BER performance on the 16-ary QAM obtained by the link-level simulation, where uncorrelated fading, second-order diversity, and coherent detection were assumed. The BER tables for various values of the Rician K-factors and the received SIRs were obtained from these preliminary simulations.

Figure 3 shows the beam throughput and the size of active beam set according to the pilot SIR threshold ratio for the user reporting when 400 users are uniformly distributed in the service area and Max SIR scheduling is used. The active beams refer to ones included in the user report, which are decided as described in section III.2. It is obvious that the throughput is high when the pilot SIR threshold ratio is large. This is because the resource allocation can estimate the interbeam interference from neighboring beams more exactly. However, the higher threshold makes the user measurement report for more beams, and this leads to increasing signaling overhead in the reverse link. A value of around 20 dB is appropriate for the pilot SIR threshold ratio because it would be desirable if the system has the highest throughput, requiring the report on the smallest number of beams.

Figure 4 shows the throughput as a function of the report period for two cases of a bent-pipe satellite and a satellite with on-broad processing capability. We assume that in the case of the on-broad processing satellite, the allocation center is located at the satellite. In this case, the round-trip delay between the center and users becomes half of that in the case of the bent-pipe satellite. There is a little throughput difference between the two cases as well as different report periods. This is because the fading weakens not only the desired signal but also the interference signal. This means that even though the fading status changes, the received SIR remains at almost the same value. Therefore, packet reception quality mainly depends on the interference situations that are closely related to user location within the beam coverage, rather than on the fading state.

From the above investigation, we remark that in satellite communications, a fast measurement reporting is not so critical for adaptive transmission, unlike in terrestrial systems. This is valid when the interference power is larger than the background noise power. However, when the system load is light, the received SIR mainly depends on the fading status because the interference can be ignored in the received SIR. In this situation, the long round-trip delay of the satellite system causes a performance degradation of the adaptive transmission. We will see this in Fig. 6.

Figure 5 shows the beam throughput according to the off-axis loss at the beam edge, which represents the size of the beam coverage. There is an optimal coverage size according to the beam pattern because of a trade-off between antenna gain loss and interbeam interference. In Fig. 5, the optimal off-axis loss becomes around 15 dB.

For the given antenna patterns, however, increasing the off-axis loss at the beam edge enlarges the beam coverage, which results in a decrease of the capacity per unit area even though the capacity per beam increases. Furthermore, the large coverage may cause a severe unfairness for user services due to the packet scheduling. This will be addressed later with the simulation results for the scheduling schemes.

Figure 6 shows beam throughput versus packet delay performance for the four scheduling schemes defined by Table 1. The dotted line denotes a 95-percentile delay defined as a

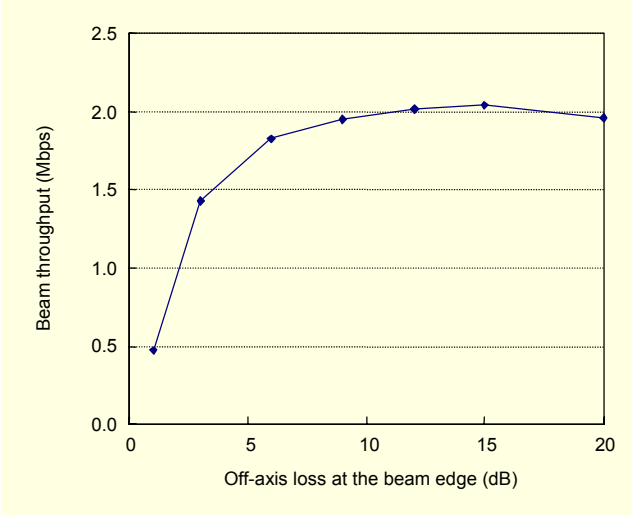

Fig. 5. Beam throughput according to the cell size (Max SIR scheduling, 400 users).

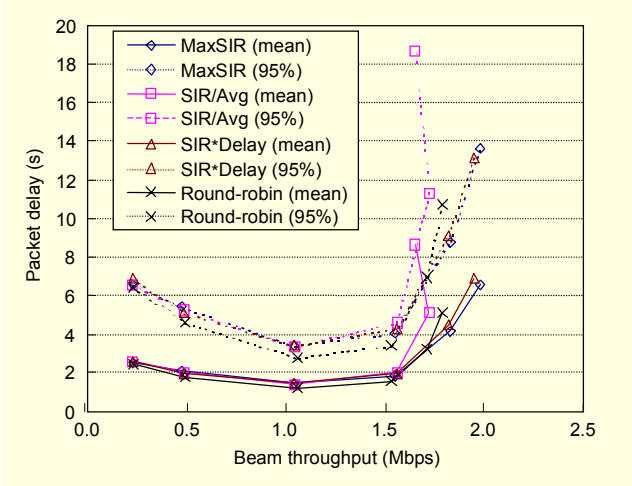

Fig. 6. Throughput-delay performance for the four scheduling schemes.

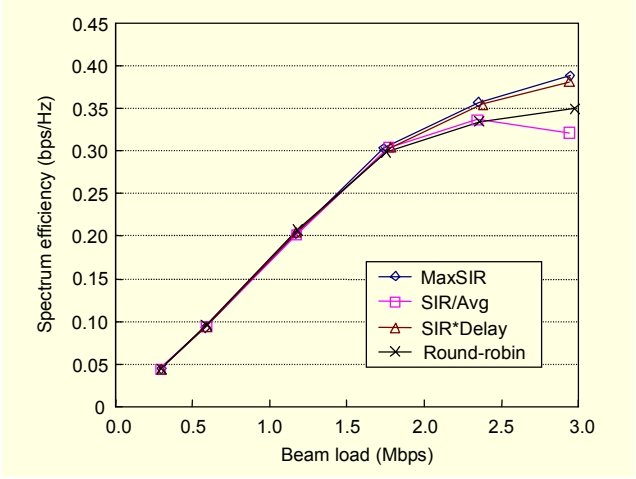

Fig. 7. Spectrum efficiency for the four scheduling schemes.

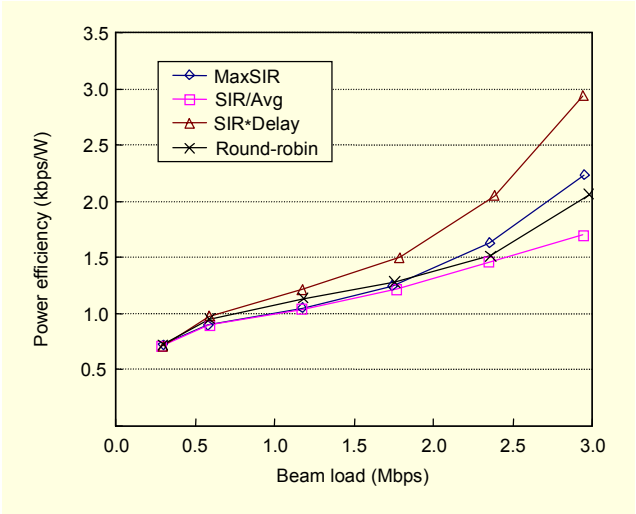

Fig. 8. Average beam power efficiency for the four scheduling schemes.

value of t_d that satisfies Pr[delay $\leq t_d$] = 0.95, where $P_r[x \leq X]$ stands for the probability that x is equal to or smaller than X. As mentioned previously, when the beam load is light, the noise power is much larger than the interference, and thus the fading affects the received SIR variation. This leads to a loss of throughput performance because the satellite system cannot immediately adapt to the SIR variation. Therefore, in Fig. 6, the packet delay in light load conditions is rather large compared with that in medium load conditions where the SIR variation is smaller because of the dominant interference.

Figures 7 and 8 show the spectrum and power efficiencies for the different scheduling schemes. When we compare the efficiencies of scheduling schemes, including the throughput-delay performance in Fig. 6, the SIR-based scheduling schemes of Max SIR and SIR*Delay outperform the round-robin scheduling. The SIR/Avg scheduling may provide a proportional fair scheduling because it gives a higher transmission priority to a user whose current channel condition improves compared with the average channel condition. However, the SIR/Avg scheduling shows the worst performance.

We compared the capacities of the proposed synchronous and conventional asynchronous systems. Figure 9 shows the normalized capacity of both systems as a function of the required SIR per symbol, γ_u^*, and the interference factor, κ_{oc}. The capacity is defined by the number of packets successfully received in a slot, and it is normalized by a spreading factor of 16. Clearly, the results indicate that the capacity difference between the two systems increases as the interference factor decreases, and that the synchronous system has at least two times a larger capacity. The interbeam interference in the

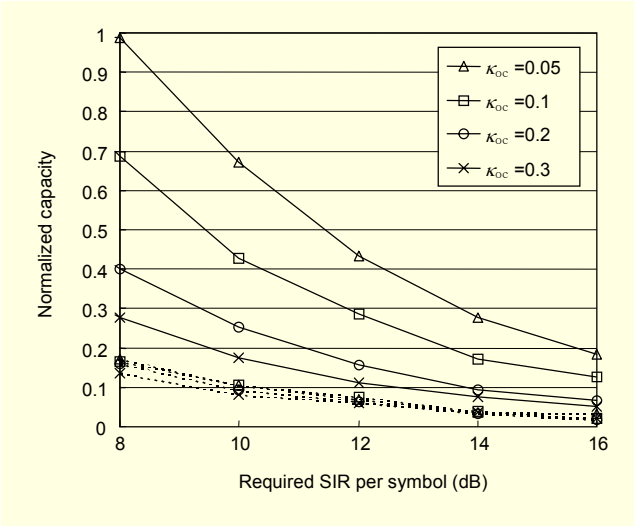

Fig. 9. Capacity comparison of the synchronous (solid line) and asynchronous (dotted line) systems (Max SIR scheduling).

synchronous system is less severe than that in the asynchronous system since the adjacent beams in the synchronous system use and share different orthogonal spreading codes in the same slot. If the channel is not frequency-selective, we can expect an interference factor close to zero, and the capacity of the synchronous system will not be limited by the interference from signals using different codes. Meanwhile, there is very little difference in the capacity of the asynchronous system according to the interference factor. This is because the interbeam interference is a dominant impairment in the conventional asynchronous system.

V. Conclusion

In this paper, we presented an efficient adaptive radio resource allocation scheme for mobile packet services in a synchronous multibeam GSO satellite system. The proposed method provides dynamic radio resource sharing and an adaptation to traffic and interference variation. This makes it possible to improve the system throughput at the expense of computational load.

Simulation results pointed out that the proposed synchronous system shows more than double the capacity compared with the conventional asynchronous system. In the multibeam GSO satellite system, the instantaneous measurement and report-on-channel conditions from users is not critical for improving the system throughput because of the long round-trip delay and identical multibeam path for each user. The system-level adaptation and allocation according to packet traffic and mutual interference among users is more useful for improving the system throughput. In the comparison of various scheduling schemes, the scheduling scheme jointly considering the SIR and the packet delay would be more attractive from the perspective of performance and fairness.

In this paper, we did not consider a few factors, leaving them for further studies. The rain attenuation effect in the channel model should be considered in the future because it is one of the most important factors degrading satellite link quality in high frequency bands. We also need to compare the system performance using various types of allocation methods.

References

[1] Shunichiro Egami, "A Power-Sharing Multiple-Beam Mobile Satellite in Ka Band," *IEEE J. Select. Areas Commun.*, vol. 17, no. 2, Feb. 1999, pp. 145-152.

[2] Seung Keun Park, Pyung Dong Cho, Ki Shik Park, and Kyung Rok Cho, "Approximating the Outage Probability of the Pilot Channel for IS-95-Based Cellular CDMA Systems in the Soft Handover Region," *ETRI J.*, vol. 25, no. 6, Dec. 2003, pp. 523-526.

[3] Javier Romero-Garcia and Riccardo De Gaudenzi, "On Antenna Design and Capacity Analysis for the Forward Link of a Multibeam Power Controlled Satellite CDMA Network," *IEEE J. Select. Areas Commun.*, vol. 18, no. 7, July 2000, pp. 1230-1244.

[4] Kwangjae Lim and Sooyoung Kim, "Downlink Radio Resource Allocation for Multibeam Satellite Communications," *Electron. Lett.*, vol. 39, no. 11, May 2003, pp. 871-872.

[5] Seong-Jun Oh and Kimberly M. Wasserman, "Dynamic Spreading Gain Control in Multiservice CDMA Networks," *IEEE J. Select. Areas Commun.*, vol. 17, no. 5, May 1999, pp. 918-927.

[6] Joon Bae Kim and Michael L. Honig, "Resource Allocation for Multiple Classes of DS-CDMA Traffic," *IEEE Trans. Veh. Technol.*, vol. 49, no. 2, March 2000, pp. 506-519.

[7] Doru Calin and Marc Areny, "Impact of Radio Resource Allocation Policies on the TD-CDMA System Performance: Evaluation of Major Critical Parameters," *IEEE J. Select. Areas Commun.*, vol. 19, no. 10, Oct. 2001, pp. 1847-1859.

[8] Kwang Jae Lim, Kyung Sup Kwak, Seog Gyu Kim, and Sun Park., "Medium Access and Radio Link Control Algorithms for Mobile Multimedia CDMA," *J. Communications and Networks*, vol. 1, no. 4, Dec. 1999.

[9] Matthew Andrews et al, "Providing Quality of Service over a Shared Wireless Link," *IEEE Commun. Mag.*, Feb. 2001, pp. 153-154.

[10] Roy D. Yates, "A Framework for Uplink Power Control in Cellular Radio Systems," *IEEE J. Select. Areas Commun.,* vol. 13, no. 7, Sep. 1995, pp. 1341-1347.

[11] Fernando Pérez Fontán, Maryan Vázquez-Gastro, Cristina Enjamio Cabado, Jorge Pita García, and Erwin Kubista, "Statistical Modeling of the LMS Channel," *IEEE Trans. Veh. Technol.*, vol. 50, no. 6, Nov. 2001, pp. 1549-1567.

[12] Third Generation Partnership Project (3GPP), "Physical Layer Aspects of UTRA High Speed Downlink Packet Access," Technical Report 25.848, 2001.

Kwangjae Lim received the BS, MS, and PhD degrees in electronics engineering from Inha University, Korea, in 1992, 1994 and 1999. In March 1999, he joined ETRI, Korea, as a Senior Member of Research Staff. Since 1999, he has worked on the standardization on IMT-2000 and has been charged with the working group on satellites under the project group on IMT-2000 and systems beyond at Telecommunications Technology Association (TTA), Korea. His recent work has been on standardization and design for IEEE 802.16 and High-speed Portable internet (HPi). His research interests are in adaptive transmission and radio resource allocation in mobile and wireless communication systems.

Sooyoung Kim received the BS degree in electrical and electronics engineering from Korea Advanced Institute of Science and Technology, Korea, in 1990. After having worked in the Satellite Communication Technology Division, ETRI, Korea from February 1990 to September 1991, she received the MSc and the PhD degrees in electrical and electronics engineering from University of Surrey, U.K in 1992 and 1995. From November 1994 to June 1996, she was employed as a research fellow at the Centre for Satellite Engineering Research, University of Surrey, U.K. In 1996 she re-joined ETRI, and worked as the Team Leader of "Broadband Wireless Transmission Team." She is now in a faculty position in the Division of Electronics & Information Engineering, Chonbuk National University, Korea. She is interested in developing highly efficient coding and modulation techniques for digital communication systems.

Ho-Jin Lee received the BS, MS, and PhD degrees in electronics engineering from Seoul National University, Seoul, Korea, in 1981, 1983, and 1990. He joined ETRI in 1983 and has been involved with satellite communication R&D since 1990. He is currently the Director of the Satellite Communications Group. His recent work has been with DVB-RCS VSAT and mobile satellite Internet access systems development. His research interests include mobile broadband satellite communication and convergence of satellite communication and broadcasting. He has been serving as the Satellite Comm. Committee Chair of KICS since 2002.